

和频、差频共存的太赫兹波上转换探测理论分析

尹晓琴¹, 范书振^{1,2,*}, 李永富^{1,2}, 张行愚^{1,3}, 刘兆军^{1,3}, 赵显^{1,2}, 方家熊^{1,2,4}¹ 山东大学激光与红外系统集成技术教育部重点实验室, 山东 青岛 266237;² 山东大学光学高等研究中心, 山东 青岛 266237;³ 山东大学信息科学与工程学院, 山东 青岛 266237;⁴ 中国科学院上海技术物理研究所, 上海 200083

摘要 基于非线性频率上转换的太赫兹波探测技术具有灵敏度高、响应速度快、可室温操作等优点, 现有理论研究中仅考虑了差频转换或和频转换, 而这与实验中观察到的二者共存的物理现实并不一致。本文提出了在非线性频率转换过程中差频与和频共存时的理论方程, 并以 DAST 晶体为例模拟分析了不同晶体厚度及泵浦强度下的太赫兹波探测情况。理论计算表明: 和频、差频共存下各波变化趋势与单差频或单和频情况有所不同; 和频过程的存在会降低差频过程的效率, 若只考虑差频, 则结果将有所偏差。在特定实验条件下, 同时利用差频光与和频光, 总信号输出强度更大, 其探测效率高于单差频的情况; 存在一个最佳的晶体厚度, 使得总信号输出最强。进一步计算表明, 基于非线性频率上转换的太赫兹单光子探测有可能实现。

关键词 非线性光学; 上转换; 差频与和频共存; 太赫兹波探测; 单光子探测

中图分类号 O441.4

文献标志码 A

doi: 10.3788/CJL202148.1214001

1 引言

近年来, 太赫兹 (THz) 技术蓬勃发展, 在物体成像、环境监测、医疗诊断、卫星通信和雷达等领域发挥着重要作用, 有着良好的应用前景^[1-5]。其中, 实现对太赫兹波的高灵敏室温探测仍是太赫兹技术发展的重要研究方向。

现有太赫兹波探测器依据物理机制可分为五大类: 太赫兹波加热材料使其物理性质发生变化; 太赫兹波与电子的集体运动相互作用; 太赫兹波诱发电子跃迁; 太赫兹波与参考辐射在非线性介质中作用; 太赫兹波与超短光脉冲相互作用^[6]。基于太赫兹波和参考辐射在非线性介质中作用的频率上转换探测技术是一种很有发展前景的太赫兹波探测技术, 利用晶体的二阶非线性效应, 近红外泵浦光和太赫兹光差频或和频可产生另外一束近红外光, 此近红外光与入射太赫兹光有一定的对应关系, 因此可以使用近红外波段成熟的高灵敏度探测技术, 通过探测

近红外光的方式间接实现太赫兹波的高灵敏度探测。通常, 此技术可采用低成本的调 Q 激光器作为泵浦光, 可在室温下操作, 具有高灵敏度、快速响应 (纳秒量级)、频率可调等良好性能。太赫兹领域的频率上转换技术近年来发展迅速, 使用 LiNbO₃、GaAs、GaSe、ZnGeP₂、GaP 等晶体均能实现高灵敏度探测^[7-9]。有机晶体 DAST, 因其非线性极化系数大、对太赫兹吸收低等特性, 在太赫兹领域得到了广泛应用, 已有研究实现了高灵敏的太赫兹波探测^[10-11] 及太赫兹实时成像^[12]。

非线性频率上转换探测方式一般可分为差频方式与和频方式。对于太赫兹波探测, 一般采用差频方式, 这与差频过程中产生太赫兹波、和频过程消耗太赫兹波有关, 且差频方式的转化效率较和频方式高。针对基于差频过程的太赫兹波频率上转换探测, 已有报道在理论和实验方面分析了探测的最优条件, 并探索了极微弱太赫兹波探测与成像的可行性^[13-14]。但是, 对基于共线相位匹配架构的太赫兹

收稿日期: 2021-03-01; 修回日期: 2021-03-26; 录用日期: 2021-04-19

基金项目: 国家自然科学基金(61775122, 12074222)、山东省自然科学基金面上项目(ZR2017MF038)

*E-mail: fanshuzhen@sdu.edu.cn

波探测而言,近红外光和太赫兹光在很宽的谱段内均能实现准相位匹配。因此,当同一泵浦光入射时,差频与和频过程通常同时存在,在实验中亦可观察到此现象^[15]。此时,光波实际作用规律及探测优化条件将与理论上单一考虑差频过程有所差异,这仍需进行进一步理论研究。

本文主要分析和频、差频共存下的光波相互作用过程,即泵浦光和太赫兹光入射到非线性晶体中同时发生的差频与和频过程。基于三波耦合方程推导得到和频、差频共存下光波相互作用方程,同时以非线性有机晶体 DAST 为例进行模拟分析。为了更好地展示 3 种不同机理下(单差频,单和频,和频、差频共存)太赫兹波及上转换光的变换规律,本文对理想情况进行了数值模拟与对比;并结合已有的实验参数,分析泵浦强度及晶体厚度对实际探测结果的影响并进行优化设计。最后,对和频、差频共存下的太赫兹单光子探测进行模拟计算,为之后的实验提供一定的理论指导。

2 基本原理

图 1 为非线性频率上转换太赫兹波探测的基本原理及实验框图。近红外泵浦光和太赫兹光共线入射到非线性晶体中并相互作用,经差频或和频转换

可产生另外一束近红外光,产生的信号光经滤波处理后被探测器接收,通过测量与分析信号光即可确定入射太赫兹波的特性,进而利用近红外波段成熟的高灵敏度探测技术间接实现太赫兹波的高灵敏度探测。

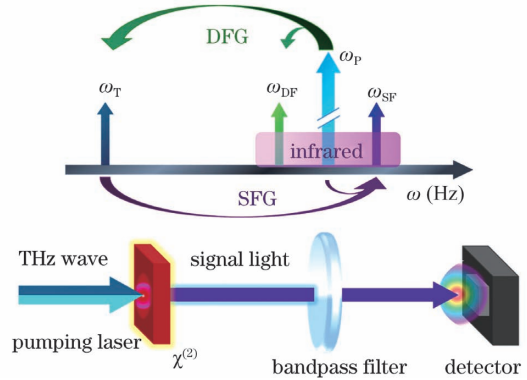


图 1 非线性频率上转换太赫兹波探测原理及实验框图

Fig. 1 Principle and experimental block diagram of terahertz-wave frequency up-conversion detection

频率上转换探测理论是基于二阶非线性效应,由耦合波方程描述。考虑到非线性频率转换中差频过程与和频过程的共同存在,本研究对经典的三波耦合方程,即慢变幅近似下的波动方程^[16]进行改进与进一步推演,从而得到和频、差频共存下的光波相互作用方程

$$\frac{d}{dz}A_P(z) = -\frac{\alpha_P}{2}A_P(z) + \frac{i\omega_P\chi_{eff}}{n_Pc}A_T(z)A_{DF}(z)\exp(-i\Delta k_1z) + \frac{i\omega_P\chi_{eff}}{n_Pc}A_{SF}(z)A_T^*(z)\exp(i\Delta k_2z), \quad (1)$$

$$\frac{d}{dz}A_T(z) = -\frac{\alpha_T}{2}A_T(z) + \frac{i\omega_T\chi_{eff}}{n_Tc}A_P(z)A_{DF}^*(z)\exp(i\Delta k_1z) + \frac{i\omega_T\chi_{eff}}{n_Tc}A_{SF}(z)A_P^*(z)\exp(i\Delta k_2z), \quad (2)$$

$$\frac{d}{dz}A_{DF}(z) = -\frac{\alpha_{DF}}{2}A_{DF}(z) + \frac{i\omega_{DF}\chi_{eff}}{n_{DF}c}A_P(z)A_T^*(z)\exp(i\Delta k_1z), \quad (3)$$

$$\frac{d}{dz}A_{SF}(z) = -\frac{\alpha_{SF}}{2}A_{SF}(z) + \frac{i\omega_{SF}\chi_{eff}}{n_{SF}c}A_P(z)A_T(z)\exp(-i\Delta k_2z), \quad (4)$$

式中: z 为作用距离; c 为光速; n 为折射率; ω 为频率; A 为光振幅; α 为晶体吸收率; χ_{eff} 为晶体的有效非线性极化率(例如 DAST 晶体中,一般取 $\chi_{eff} = 490 \text{ pm/V}^{[17]}$); Δk 为相位失配量, $\Delta k_1 = k_P - k_T - k_{DF}$, $\Delta k_2 = k_{SF} - k_P - k_T$;下标 P、T、DF 与 SF 分别代表泵浦光、太赫兹光、差频信号光与和频信号光。差频信号光由泵浦光和太赫兹波差频产生,和频光由二者和频产生。

3 分析与讨论

对于耦合波动方程,和频、差频相互作用与各波

参数的关系复杂,难以通过公式计算得出解析解,在此仅提供数值模拟。以非线性有机晶体 DAST 为例,设各光偏振方向均沿 DAST 晶体 a 轴,基于平面波近似与共线相互作用,模拟和频、差频共存下的光波相互作用方程并进行相关性分析,各波的相关参数来自文献^[18-19]。

为了直观地展示不同非线性过程中太赫兹波及上转换光的变换规律,首先对理想情况下(忽略晶体对光的吸收及相位失配的影响)微弱太赫兹波探测的和频、差频共存时光波相互作用过程进行了数值模拟,并与单差频及单和频过程进行了比较,结果如

图 2 所示。可以看到:在单差频过程中,泵浦光的光子数减少甚微,太赫兹光和上转换差频光的光子数呈指数式增加,满足曼利-罗 (Manley-Rowe) 关系,太赫兹光子增加量和泵浦光子减少量相等,且与上转换光子增加量相等;在单和频过程中,泵浦光与太赫兹光的光子数同步减少,上转换和频光的光子数等量增加,即两个光子能量转化成一個和频光子能量,同样满足曼利-罗关系;对于差频与和频共存的情况,太赫兹光子数量有一定的减少,但变化极为微弱,上转换差频光与和频光同时增强,和频光子数略高于差频光子数。四波光子数间的关系为:泵浦光子减少量等于差频光子增加量与和频光子增加量之和,上转换和频光子增加量等于上转换差频光子增加量与太赫兹光子减少量之和。同时,从图 2 亦可明显看出太赫兹波在 3 个过程的不同变化情况:当差频与和频共存时,太赫兹波变化微弱,既没有出现单差频过程中的迅速上升现象,也不会像单和频过程一样快速下降。

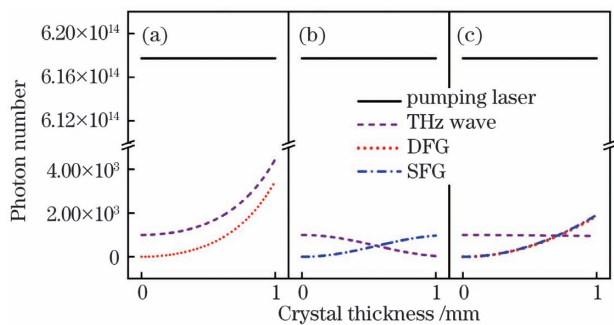


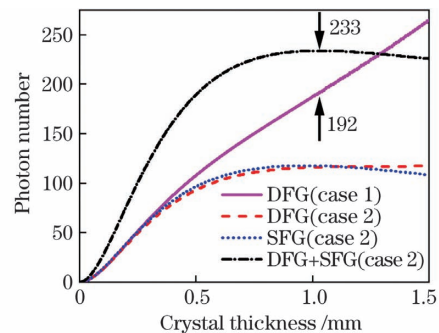
图 2 理想情况下各波在 DAST 晶体中的演变过程。

(a) 单差频; (b) 单和频; (c) 差频与和频共存

Fig. 2 The evolution of all waves within a DAST crystal in ideal conditions. (a) Only DFG considered; (b) only SFG considered; (c) coexistence of DFG and SFG

为了探究微弱太赫兹波探测的实际情况,使理论模拟结果对实验更具有指导意义,考虑晶体对光的吸收以及相位失配的影响,将与波长相关的吸收系数 ($\alpha_P = \alpha_{DF} = \alpha_{SF} = 150 \text{ m}^{-1}$, $\alpha_T = 7300 \text{ m}^{-1}$) 和相位失配量 $\Delta k_1 = 2\pi \left(\frac{n_P}{\lambda_P} - \frac{n_T}{\lambda_T} - \frac{n_{DF}}{\lambda_{DF}} \right)$, $\Delta k_2 = 2\pi \left(\frac{n_{SF}}{\lambda_{SF}} - \frac{n_P}{\lambda_P} - \frac{n_T}{\lambda_T} \right)$ 加入到模拟计算中^[18-19]。同时基于已有的实验结果^[11], 设置泵浦光强度为 28 MW/cm^2 , 入射太赫兹光子数为 10^3 个, 模拟和频、差频共存下的信号光变化过程, 同时与单差频情况进行对比分析。在基于 DAST 晶体非线性频率上转换的典型波段 4.3 THz ^[20] 中, 泵浦波长采用差

频过程对应的相位匹配波长 1395 nm , 得到两种不同机理下的信号光变化情况, 如图 3 所示。其中, 相位匹配波长由最大相干长度 (最小相位失配量) 确定, 其计算公式为 $l_c = \frac{\pi}{|\Delta k|}$, 与三波的波长及折射率等参数有关^[13]。从图 3 可以看到: 单差频过程中, 晶体厚度越大, 转换效率越高; 当差频与和频共存时, 存在最佳晶体厚度使得总的上转换信号光的输出最强。各波相互作用初始, 和频过程与差频过程的效率相当, 但经过光波相互转换及一定距离的晶体吸收后, 在 1 mm 附近太赫兹光太弱, 差频过程产生的太赫兹光已无法维持泵浦光与太赫兹光的和频正向转换, 出现逆转换现象, 和频光子数开始下降; 对其中的差频过程而言, 泵浦光较强, 足以维持该过程正向转换, 但因太赫兹光较弱, 转换效率较低, 差频光子数缓慢增加, 使得总信号光子数存在最大值。在上述实验条件下, 当晶体厚度为 1.03 mm 时可获得最大的总信号光 (差频光与和频光之和) 输出, 光子数为 233 个, 多于单差频过程的信号光子数 192 个, 总的可探测信号光子数有所增加, 即同时利用差频过程与和频过程, 探测效率理论上可相对提高约 18%。此时, 和频、差频共存下的差频光子数为 116 个, 少于单差频情况下的信号光子数。因和频过程会消耗太赫兹光子, 其存在会导致相应差频过程的转换效率降低, 这就很好地解释了差频输出功率的衰减现象。此外, 和频、差频共存情况下的总输出在最佳厚度附近变化缓慢, 对于 $0.85 \sim 1.27 \text{ mm}$ 厚度范围内的晶体, 总信号光子数为 (232 ± 1) 个。即在上述实验条件下, 总信号光强度变化对晶体厚度不十分敏感, 使用一定厚度范围内的晶体均可实现较强的总上转换信号光输出。



case 1—only DFG considered; case 2—coexistence of DFG and SFG.

图 3 微弱太赫兹波探测中信号光子数随晶体长度的变化关系

Fig. 3 Photon numbers of signal lights as functions of crystal thickness for weak terahertz-wave detection

考虑到泵浦光强度对探测效率的影响,不同泵浦功率密度下微弱太赫兹波探测情况(入射太赫兹光子数为 10^3 个)的理论模拟曲线如图 4 所示。图 4(a)描绘了和频、差频共存时 28 MW/cm^2 和 280 MW/cm^2 泵浦强度下的差频过程与和频过程。可以看到,作用初始和频、差频信号光转换效率相近。经一定距离的晶体吸收后,太赫兹光子数减少,差频产生的太赫兹光在较弱泵浦条件下(28 MW/cm^2)不足以维持和频光子数增长,和频过程逆转换;而强泵浦下(280 MW/cm^2)差频产生的太赫兹光仍可维持和频光子数继续增加,同时和频正向转换导致差频转换效率进一步降低。基于泵浦强度对差频与和频过程转换效率的影响,可得到不同泵浦强度下,常用的 1 mm 晶体内和频、差频共存时的总信号光的光子数随太赫兹光子数的变化情况,如图 4(b)所示。

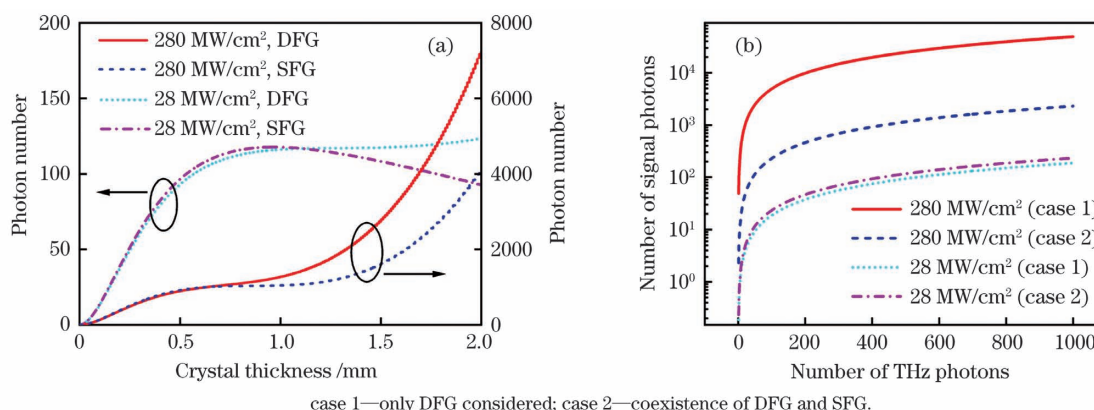


图 4 不同泵浦强度下的信号光子数的变化。(a)和频、差频共存时差频与和频信号光的光子数随晶体厚度的变化;(b)总信号光的光子数随入射太赫兹光子数的变化

Fig. 4 Photon numbers of signal lights at different pumping intensities. (a) DFG and SFG signal lights versus crystal thickness under the coexistence of DFG and SFG; (b) total photon numbers of signal lights as functions of THz photon numbers

进一步探讨和频、差频共存时的太赫兹单光子探测情况,引入探测器[如单光子探测器(SPD)、雪崩光电二极管(APD)等]的参数,考虑实际探测器噪声的影响后进行理论模拟。晶体长度设为 1 mm ,入射的太赫兹光子数设为 1,使用 SPD 进行太赫兹单光子探测的计算结果如图 5 所示。由图 5 可知,在太赫兹单光子入射情况下想要获得单光子信号光,所需的最小泵浦强度为 125 MW/cm^2 (远小于 DAST 晶体的损伤阈值 2.71 GW/cm^2 ^[21]),即使用 SPD 进行频率上转换的太赫兹单光子探测是可行的。若进一步考虑用 APD 进行探测,以美国 Voxel 公司生产的 Siletz VFP1-NKAB 型号的 InGaAs APD 为例,相关参数响应率、结电容、噪声电流密度分别为 40.4 A/W 、 1.86 pF 和 $2.412 \text{ pA/Hz}^{1/2}$,结合为使读

出噪声最小而设计的 $10 \text{ k}\Omega$ 跨阻放大及 20 倍的二阶电压放大,可计算得到其总噪声及等效噪声功率密度 D_{NEP} 分别为 12.5 mV 和 $0.155 \text{ pW/Hz}^{1/2}$,进而由 $R_{\text{SNR}} = \frac{S}{N} = \frac{S_{\text{Photon}} \cdot h\nu / T}{D_{\text{NEP}} \cdot \sqrt{D_{\text{BW}}}}$ 可计算得到信噪比,其中脉宽 $T = 10 \text{ ns}$,带宽 $D_{\text{BW}} = 100 \text{ MHz}$ 。图 5 同样展示了使用 APD 探测时其信噪比随泵浦功率的变化,考虑和频、差频共存时,使用 APD 实现太赫兹单光子探测所需的最小泵浦功率密度为 2.14 GW/cm^2 ,因其接近 DAST 的损伤阈值,在实验中较难实现。

同理,结合实际近红外相机参数,也可进一步对太赫兹单光子成像的可行性进行计算与分析,对基于非线性频率上转换技术的太赫兹单光子成像提供

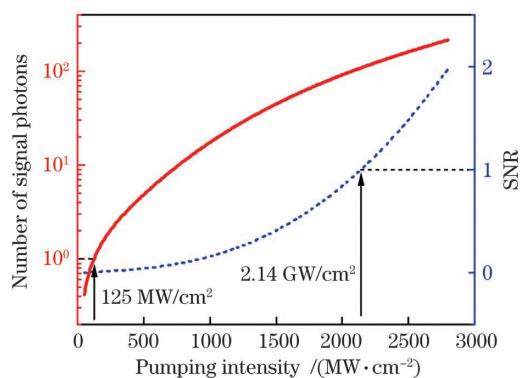


图 5 太赫兹单光子探测下的信号光子数及信噪比随泵浦光功率密度的变化

Fig. 5 The number of signal photons and the SNR as functions of the pumping power density in terahertz single-photon detection

一定的理论指导。

4 结 论

利用非线性频率上转换进行太赫兹波探测时,差频过程与和频过程同时存在。本研究在经典耦合波方程的基础上,推导并提出了和频、差频共存下的光波相互作用方程,探讨了基于 DAST 晶体的频率上转换探测情况,并针对理想情况进行分析,以便研究其相互作用过程。和频、差频共存下各波变化趋势不同于单差频或单和频情况,但均满足曼利-罗关系。同时,结合已有实验设置合适参数值,模拟微弱太赫兹波探测时的实际信号光输出,分析泵浦强度及晶体厚度对差频过程与和频过程的影响,并与仅考虑差频情况进行对比。在特定实验条件下差频与和频信号光的总强度更大,其总探测效率可高于单差频情况;且可计算得到使得总信号输出最强的最佳晶体厚度。最后,将此理论结合实际探测的噪声,进一步对单光子探测进行计算与分析,结果表明基于非线性频率上转换的太赫兹单光子探测有望实现。以上通过理论模拟所得的和频、差频共存下的太赫兹波探测情况,对以后的实验具有指导意义。

参 考 文 献

[1] Sakai K. Terahertz optoelectronics. Topics in applied physics[M]. Heidelberg: Springer, 2005, 97: 203-377.

[2] Dragoman D, Dragoman M. Terahertz fields and applications[J]. Progress in Quantum Electronics, 2004, 28(1): 1-66.

[3] Fu Z L, Li R Z, Li H Y, et al. Progress in biomedical imaging based on terahertz quantum

cascade lasers[J]. Chinese Journal of Lasers, 2020, 47(2): 0207014.

符张龙, 李锐志, 李弘义, 等. 基于太赫兹量子级联激光器的生物医学成像研究进展[J]. 中国激光, 2020, 47(2): 0207014.

- [4] Zhang X, Zhao Y M, Deng C, et al. Study on the passive terahertz image target detection [J]. Acta Optica Sinica, 2013, 33(2): 0211002.
张馨, 赵源萌, 邓朝, 等. 被动式太赫兹图像目标检测研究[J]. 光学学报, 2013, 33(2): 0211002.
- [5] Liu Y D, Xu Z, Hu J, et al. Research on quality of agricultural products by terahertz spectroscopy [J]. Laser & Optoelectronics Progress, 2021, 58(1): 0100005.
刘燕德, 徐振, 胡军, 等. 太赫兹光谱检测技术对农产品品质检测的研究进展[J]. 激光与光电子学进展, 2021, 58(1): 0100005.
- [6] Lewis R A. A review of terahertz detectors [J]. Journal of Physics D, 2019, 52(43): 433001.
- [7] Guo R X, Ohno S, Minamide H, et al. Highly sensitive coherent detection of terahertz waves at room temperature using a parametric process [J]. Applied Physics Letters, 2008, 93(2): 021106.
- [8] Khan M J, Chen J C, Kaushik S. Optical detection of terahertz radiation by using nonlinear parametric upconversion [J]. Optics Letters, 2007, 32(22): 3248-3250.
- [9] Ding Y J. Selection of optimum nonlinear crystals for efficient parametric generation and sensitive detection of monochromatic ns THz pulses [J]. MRS Online Proceedings Library, 2007, 1016(1): 201.
- [10] Minamide H, Zhang J, Guo R X, et al. High-sensitivity detection of terahertz waves using nonlinear upconversion in an organic 4-dimethylamino-N-methyl-4-stilbazolium tosylate crystal [J]. Applied Physics Letters, 2010, 97(12): 121106.
- [11] Qi F, Fan S Z, Notake T, et al. 10 aJ-level sensing of nanosecond pulse below 10 THz by frequency upconversion detection via DAST crystal: more than a 4 K bolometer [J]. Optics Letters, 2014, 39(5): 1294-1297.
- [12] Fan S Z, Qi F, Notake T, et al. Diffraction-limited real-time terahertz imaging by optical frequency upconversion in a DAST crystal [J]. Optics Express, 2015, 23(6): 7611-7618.
- [13] Yin X Q, Liu J L, Fan S Z, et al. Theoretical exploration of terahertz single-photon detection and imaging by nonlinear optical frequency up-conversion [J]. Journal of Infrared, Millimeter, and Terahertz Waves, 2020, 41(10): 1267-1279.
- [14] Qi F, Fan S Z, Notake T, et al. An ultra-broadband

- frequency-domain terahertz measurement system based on frequency conversion via DAST crystal with an optimized phase-matching condition [J]. *Laser Physics Letters*, 2014, 11(8): 085403.
- [15] Pfeiffer T, Kutas M, Haase B, et al. Terahertz detection by upconversion to the near-infrared using picosecond pulses [J]. *Optics Express*, 2020, 28(20): 29419-29429.
- [16] Shen Y R. *Nonlinear infrared generation* [M]. Heidelberg: Springer, 1977: 19-133.
- [17] Schneider A, Stillhart M, Günter P. High efficiency generation and detection of terahertz pulses using laser pulses at telecommunication wavelengths [J]. *Optics Express*, 2006, 14(12): 5376-5384.
- [18] Jazbinsek M, Mutter L, Günter P. Photonic applications with the organic nonlinear optical crystal DAST [J]. *IEEE Journal of Selected Topics in Quantum Electronics*, 2008, 14(5): 1298-1311.
- [19] Ohno S, Miyamoto K, Minamide H, et al. New method to determine the refractive index and the absorption coefficient of organic nonlinear crystals in the ultra-wideband THz region [J]. *Optics Express*, 2010, 18(16): 17306-17312.
- [20] Ito H, Miyamoto K, Minamide H. Ultra-broadband, frequency-agile THz-wave generator and its applications [C]// *Advanced Solid-State Photonics*, January 27-30, 2008, Nara, Japan. Washington, D. C.: OSA, 2008: WD1.
- [21] Manivannan M, Dhas S A M B, Balakrishnan M, et al. Study of optical and laser damage threshold in EDTA and DTPA-doped DAST single crystals [J]. *Applied Physics B*, 2018, 124(8): 166.

Theoretical Analysis of Terahertz-Wave Frequency Up-Conversion Detection Based on Coexisting Difference- and Sum-Frequency Generation

Yin Xiaoqin¹, Fan Shuzhen^{1,2*}, Li Yongfu^{1,2}, Zhang Xingyu^{1,3}, Liu Zhaojun^{1,3},
Zhao Xian^{1,2}, Fang Jiexiong^{1,2,4}

¹Key Laboratory of Laser & Infrared System (Shandong University), Ministry of Education, Qingdao, Shandong 266237, China;

²Center for Optics Research and Engineering (CORE), Shandong University, Qingdao, Shandong 266237, China;

³School of Information Science and Engineering, Shandong University, Qingdao, Shandong 266237, China;

⁴Shanghai Institute of Technical Physics, Chinese Academy of Sciences, Shanghai 200083, China

Abstract

Objective Terahertz technology is developing rapidly and is widely used in various basic scientific research and application fields such as biology, industrial nondestructive evaluation, environment monitoring, and security. Among the various applications, high-sensitivity detection of terahertz waves has attracted considerable attention. Terahertz-wave detection technology based on nonlinear frequency up-conversion is a promising technique owing to its decent performance in terms of high sensitivity, fast response, and room-temperature operation. Based on the second-order nonlinear effect in crystals, a new near-infrared (NIR) signal light is obtained via the interaction of NIR pumping laser and terahertz wave. High-sensitivity detection of terahertz waves can be achieved with the assistance of signal light detection using mature NIR detection technology. In experiments, difference-frequency generation (DFG) and sum-frequency generation (SFG) exist together. In previous studies, only DFG or SFG process was considered, both of which possess some limitations. Therefore, the coexistence of DFG and SFG demands prompt investigation. In this study, theoretical nonlinear frequency conversion equations that contain both DFG and SFG are proposed. The detailed situations of terahertz-wave detection based on DAST crystals were simulated and analyzed under different setting conditions. Such a theoretical study of terahertz wave detection under the coexistence of DFG and SFG will be helpful in future experiments.

Methods In this study, four-wave interaction equations considering the coexistence of DFG and SFG are proposed, derived from the improvement and further deduction of classical three-wave coupling equations. Considering the nonlinear organic crystal DAST as an example, a series of simulations and analyses were performed based on the

four-wave interaction equations using MATLAB software and conclusions were drawn. To illustrate lightwave conversion in different nonlinear processes, an ideal case of ignoring the light absorption and phase mismatching was first analyzed. In the next step, considering the typical wavebands commonly used for nonlinear frequency up-conversion with DAST crystals, 4.3 THz and 1395 nm were respectively chosen as the frequency of terahertz wave and corresponding pumping wavelength in further simulations. To optimize the terahertz detection more practically, the difference- and sum-frequency processes under different pumping intensities and DAST crystal thicknesses were calculated. In addition, the simulation of terahertz single-photon detection based on the coexistence of DFG and SFG was performed.

Results and Discussions The theoretical calculation results based on the four-wave interaction equations are as follows. For the evolution of terahertz waves and up-converted signal light, three nonlinear processes (DFG, SFG, and coexistence situation) showed different characteristics. The terahertz optical intensity slightly changed with the coexistence of DFG and SFG; it neither rose rapidly in the single difference-frequency process nor did it decrease rapidly in the single sum-frequency process (Fig. 2). Considering the absorption and phase mismatching in simulations, the calculation results were more helpful in experiments. At the beginning of the interaction, the conversion efficiency of the sum- and difference-frequency processes were similar, but the terahertz intensity declined quickly under the combined action of the conversion and crystal absorption after a certain distance. When the pumping intensity was weak, the terahertz photons generated by the difference-frequency process were insufficient for continuing the sum-frequency conversion, which led to the reversion of the sum-frequency process. In addition, the signal light of the difference-frequency process increased slowly, so the total signal photon number had a maximum value corresponding to the optimal crystal thickness; the maximum output was larger than that when only the difference-frequency process was considered (Fig. 3). However, when the pumping intensity became larger, the generated terahertz wave was sufficient for maintaining the sum-frequency process and the signal light continued to increase. The efficiency of the difference-frequency conversion further decreased owing to the sum-frequency conversion. The total signal photon number was still smaller than that in the single difference-frequency process, indicating that the existence of the sum-frequency process significantly affected the difference-frequency conversion (Fig. 4). Therefore, we can choose different pumping wavelengths to change the phase matching of the two processes and improve the detection efficiency by using or suppressing the sum-frequency process.

Conclusions In terahertz-wave detection through nonlinear frequency up-conversion, the difference- and sum-frequency processes coexist. The lightwave conversion between the pumping laser, terahertz wave, and signal light satisfies the Manley-Rowe relations. The nonlinear optical evolution under the coexistence of DFG and SFG differed from that of the case where only either was considered. The existence of the sum-frequency process reduced the difference-frequency conversion efficiency. Thus, the results obtained by ignoring the concurrent sum-frequency conversion may be inaccurate. Further, both pumping intensity and crystal thickness had a significant impact on the frequency up-conversion process. The total signal intensity of DFG and SFG was higher than that when only DFG was considered, leading to a higher detection efficiency under certain experimental conditions. In addition, there was an optimal crystal thickness corresponding to the maximum total signal output. Further theoretical simulations showed that terahertz-wave single-photon detection through nonlinear optical frequency up-conversion could be realized using an NIR single-photon detector.

Key words nonlinear optics; upconversion; coexistence difference- and sum-frequency generation; terahertz-wave detection; single-photon detection

OCIS codes 190.7220; 190.4223; 040.2235; 040.3780